

OLED Based Transparent MIMO Antennas for Future 5G mm-Wave Applications

M. Asim¹, W. Batool², M. Zahid³, Y. Amin⁴, H. Tenhunen⁵

^{1,2,3,4}Department of Telecommunication Engineering, University of Engineering & Technology, Taxila, Pakistan.

⁵Department of Information Technology, University of Turku, Turku, Finland.

³muhammad.zahid@uettaxila.edu.pk

Abstract- The proposed paper offers the layout to integrate an Organic Light Emitting Diode (OLED), an optically transparent antenna for 5th Generation wireless communication. The proposed antenna is depicted on a glass substrate which has a relative permittivity $\epsilon_r=5.5$ and is optically transparent and compact. The radiative patch and a ground plane are its key components that use PEC material. The suggested antenna is a chain of small isosceles triangle cells (micrometric) placed on the substrate made of glass to attain wideband characteristics. With the assistance of triangle-shaped symmetry, the theoretical optical transparency obtained is about 95%. The antenna proposed covers the band of 39 GHz from 38.19 GHz to 40 GHz with a bandwidth of 1.81 GHz. It covers a gain of 4.263 dB and directivity of about 4.65 dB. Channel capacity and the data rate get better at the transmitter and receiver end by using an 11-element MIMO antenna on the OLED structure. Simulated results show that this antenna is applicable for 5G applications due to its transparency, low profile, flexibility, and wide achievable frequency bandwidth.

Keywords- mm-Wave, Transparent, Smartphone, MIMO, OLED

I. INTRODUCTION

The wireless verbal exchange has made noteworthy progress as it has developed through diverse generations. This evolution is characterized by the aid of the technical implementation of a specific preferred, inclusive of new techniques and functions that differentiate it from the preceding generation [1]. In the Eighties, the smartphone became democratized to the public, and all types of documentation were extinct. Mobile communication structures overcame multiple levels to increase facts price and transferring pace. These days, data charge speed reaches as much as 100Mbps/s [2]. In cities, nearly half of the world population lives (55 percent), which will rise to 68 percent by 2050, reports [3]. New demanding situations arise due to growth within the relocation of human beings to urban regions. So with the assistance of

technological advances, this makes cities more sustainable [4].

The strain is put on the current generation due to tremendous data traffic growth. It influenced to bring a new system with a higher data rate and efficient transfer speed that could accommodate billions of IoTs. The data rate of 20 Gbps is the focus for fifth-generation (5G) systems that will be the first step to constituting the smart city concept. Furthermore, while extending the battery life, ten timeless energy will be consumed[5-7].

Technological issues arise with the abrupt increase in the relocation of people to urban areas. Urban areas seek to implement artificial intelligence and smart technologies for a smart urban solution. They aim to improve and interconnect street lighting, electrical network, automotive and public transport, and much more, and it needs a larger communication area. [2],[8]. Due to lack of space, multiple base stations cannot be implanted because it may cause visual pollution. Also, to connect the internet of things system with the network, numerous antennas should be installed on these objects.

To overcome this issue, antennas with optical transparency can be integrated into existing furniture, bus stop, street lights, display screens (LCD and OLED) [9-10], and innovative watch applications [11].

A single channel bandwidth accommodates only a limited number of users. So, many experiments have been performed to accommodate more users. Using one antenna, the penetration power of the signal from the transmitter to the receiver side fades. In this regard, Multiple Input Multiple Output (MIMO) works as a liberator. Due to the stable type of communication and high rate of transmission, it is widely used. Channel capacity and the data rate get better at the transmitter and receiver end by multiplying the number of antennas. The data transfer of 4G Long-Term Evolution (LTE) 20MHz cell channel is multiple times less than 5G mm-wave [19].

In this paper, we proposed a simulation examination of a new idea along with an antenna optically invisible incorporated in an OLED source. This study is based on the mechanisms of OLED and invisible antennas without affecting their

performance. Firstly, we will focus on invisible antenna performance in the mm-Wave band for 5G. The proposed antenna configuration is primarily based on the development of antennas proposed in [12]. This antenna is incorporated into the OLED supply in the second portion.

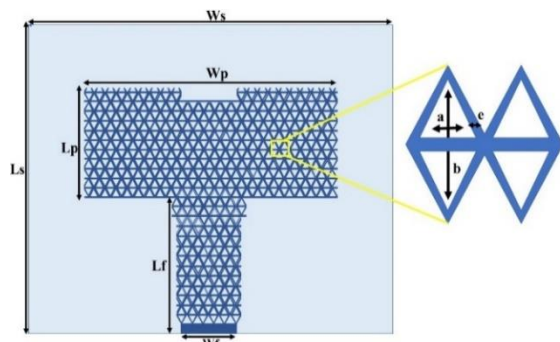
II. PROPOSED OPTICALLY TRANSPARENT ANTENNA

A. Antenna Design and Parameters

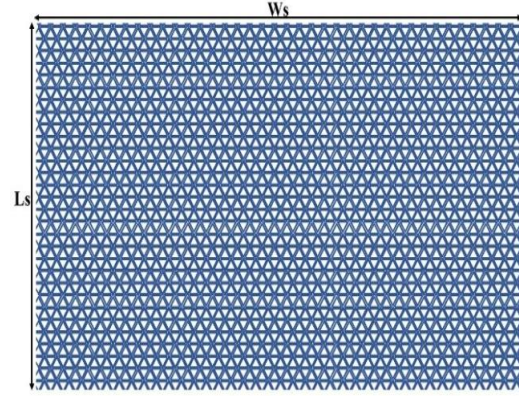
This section discusses the design and geometric configuration of an optically transparent antenna installed for 5G communication into an OLED source. Since the requirement for 5G is an mm-Wave band, the required antennas are low profile and compact. The design concept of the proposed antenna is based on a triangle grid-shaped patch antenna. The proposed antenna is designed step-by-step using the CST Microwave Studio software simulator.

This antenna comprises a glass substrate having a loss tangent $\tan\delta = 0.0054$, thickness $h_s = 480 \mu\text{m}$ and the relative permittivity of $\epsilon_r = 5.5$ with the proportion of $W_s = 5.55 \text{ mm}$ and $L_s = 4.0 \text{ mm}$. The patch ($W_p = 3.21 \text{ mm}$ and $L_p = 1.39 \text{ mm}$) is made of micrometric triangle cells placed next to each other. The ground plane is ($5.55 \times 4.0 \text{ mm}^2$) which covers the whole back side of the substrate as shown in Fig. 1. Each micrometric cell has dimensions (Fig. 1 (a)), $b = 202 \mu\text{m}$, $a = 98 \mu\text{m}$. The measure of two consecutive cells is $2 \times e$ with $e = 14 \mu\text{m}$. And the dimensions are calculated for the feed line ($W_f = 0.84 \text{ mm}$ and $L_f = 1.69 \text{ mm}$) for a higher impedance model of 50Ω .

To optimize the impedance matching and the resonant frequency, the length 'b' and the width 'a' of the triangle cell are varied.



(a) patch of the antenna and Isosceles triangle cell



(b) ground of the antenna.

Fig. 1. The configuration of the antenna.

B. Parametric study

a) The width 'a' disparity of Isosceles triangle cell:

An invariable analysis is perceived in the current section of the study to check out the antenna's performance. Fig. 2 genuinely suggests the impact of variation inside the isosceles triangle width 'a' at the reflection coefficient (S_{11}). By varying the width 'a' of the isosceles triangle, we can truly analyze the impact on the antenna consequences. In this section, parametric analysis is made based on changing the width of Isosceles triangle cells. The effect of changing width dimensions of Isosceles triangle cells on the S-parameter (S_{11}) of the proposed antenna has been shown. Three values have been considered for the cell width of the micrometric (isosceles triangle).

The antenna has been simulated for each of the three values, and the results have been analyzed. The cell width values taken into notice are ($a = 172, 180, 196 \mu\text{m}$). The micrometric cell width $a = 196 \mu\text{m}$ has been shown with a blue curve, the micrometric cell width $a = 180 \mu\text{m}$ been shown with a red curve, and the micrometric cell width $a = 172 \mu\text{m}$ has been shown with a green curve. The given Fig. 2 clearly shows that the resonant frequency value drops down to a low-frequency value with increasing width 'a'. The dip of the blue curve ($a = 196 \mu\text{m}$) is exactly at 39 GHz, while for the rest if the two values of 'a', the dip is not precisely at 39 GHz.

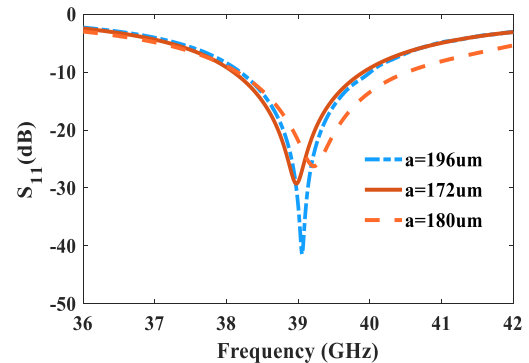


Fig. 2. S-Parameter (S_{11}) with the disparity of width 'a' of the Isosceles triangle cell.

With the increase in the parameter 'a', there is an increment in the width of radiating patch. The resonance frequency will be reduced when the width of the patch increases. Adjustments should be made to gain a desirable value so that the proposed antenna's operating band is compatible with the 39GHz band. Other than this, better optical transparency is achieved.

b) The disparity of the Isosceles triangle cell length 'b':

This part of the study focuses on the isosceles triangle length 'b' variation. It analyzes the impact of this change in the length of the isosceles triangle on the S11 parameter. The impact of changes in the isosceles triangle length 'b' on the reflection coefficient (S11) is shown in Fig. 3. Here also, three values of length 'b' have been taken into notice, and for each value of length 'b' the proposed antenna is simulated to inspect the results. The cell length values taken into notice are ($b = 200, 202, 204 \mu\text{m}$). The micrometric cell length $b = 202 \mu\text{m}$ has been shown with a blue curve, the micrometric cell length $b=204 \mu\text{m}$ has been shown with a red curve, and the micrometric cell length $b = 200 \mu\text{m}$ has been shown with a green curve.

At $b = 202 \mu\text{m}$, we obtain the result at exactly 39 GHz with a better impedance. When we increase the length 'b' of the isosceles triangle, the results deteriorate, and the antenna's bandwidth does not remain constant. From Fig. 3, we clearly notice that with the decrease in the length 'b' of the micrometric cell, a better impedance is obtained, which remains constant when the bandwidth of the desired antenna is matched.

Since varying the length of the micrometric cell changes the antenna's overall dimensions, it directly impacts the feedline. When the dimensions of the length of the cell are varied, the length of the feedline also changes. This change influences the impedance matching and gives a different outcome of parameter S11 for each value of length 'b'. Fig. 3 depicts a clear representation of the S11 parameter when the micrometric cell length 'b' is varied, and we observe three different curves, each representing lengths 'b' of 200, 202, and $204 \mu\text{m}$.

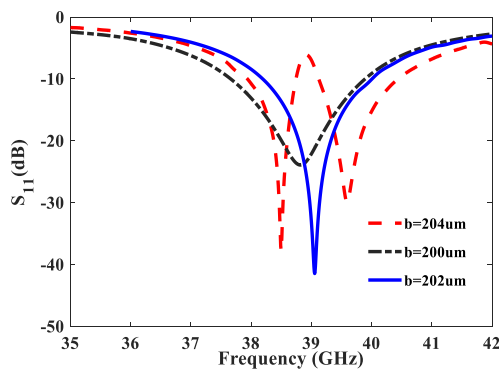


Fig. 3 S-Parameter (S11) with the disparity of length 'b' of the Isosceles triangle cell.

c) The disparity in the height of substrate:

There is a direct influence on the outcomes and performance of substrate on the working of antenna. We use glass material in the substrate as it is the core of the transparency. The substrate's thickness is a confined component in the transparency of the antenna proposed. The effect of the substrate's varying height ($h_s=480, 500, 550 \mu\text{m}$) on reflection coefficient S11 is considered and shown in Fig. 4. From the given results, it is concluded that the -10 dB reflection coefficient performance degrades with increasing substrate height, So the disparity directly impacts resonant frequency.

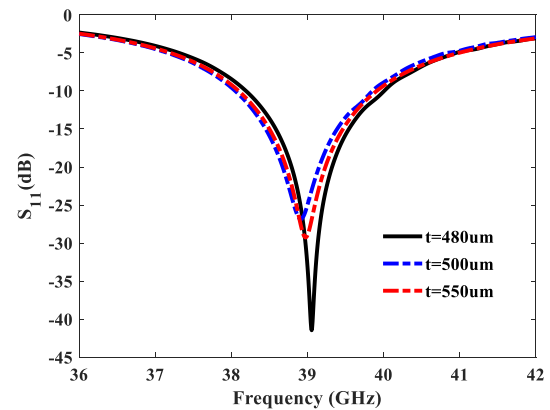


Fig. 4. S-Parameter (S11) with disparity in the height of substrate

By changing the height of the substrate, we can clearly see that the reflection coefficient changes, whereas the frequency of the antenna remains the same. By the adjustment in the height of the substrate and keeping other dimensions the same, we can obtain broadband results. In this variation, we have taken three sets of observations by changing the height of the substrate. The maximum reflection coefficient of -42dB is obtained when the height of the substrate is kept at $480\mu\text{m}$ with a maximum bandwidth of 1.81GHz . The antenna mustn't be bulky. Therefore, the height of the substrate is kept between $450\mu\text{m}$ to $550\mu\text{m}$. Moreover, the electrical characteristics are affected by the height and the dielectric of the antenna, a smaller heightened antenna will increase the bandwidth, but there might be a chance of coupling in the antenna.

C. 11-Element Transparent MIMO Antenna:

In this part of the study, the transparent and optically invisible isosceles-triangle-shaped antenna elements are extended to an 11-element array configuration to improve spectral efficiency via better spatial multiplexing. These antenna elements are integrated into the OLED structure, a sandwiched structure containing four layers, each of different materials. Fig. 5 shows the deployment of these elements on OLED structure.

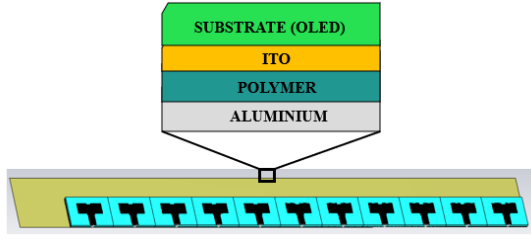


Fig. 5. 11-Element MIMO antenna integrated on OLED

The proposed antenna is configured so that a total of 11 elements of the antenna are placed in contact with each other. This 11-element antenna is integrated into OLED and is simulated to obtain the reflection coefficient (S11) parameter. The maximum isolation achieved by optically transparent invisible isosceles-triangle-shaped antenna array (11-element MIMO) is below -35dB. Fig. 6 shows the simulated S11 results of the 11-element MIMO antenna. Each MIMO element is simulated with the corresponding MIMO element to observe the reflection coefficient parameters of S1,1, S2,2 up to S11,11 parameters.

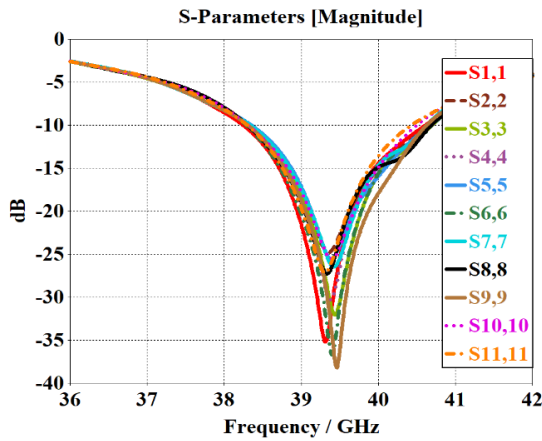


Fig. 6. S-Parameter (S11) 11-element MIMO antenna

III. INTEGRATION OF OPTICALLY TRANSPARENT ANTENNA TO OLED STRUCTURE

It is easier to fabricate Organic Light-Emitting Diodes OLEDs, so they are replacing CRTs or LED displays due to their flexibility. It gives high efficiency, operational stability, and remarkable color fidelity [8]. In the current era, researchers are notably more attracted to OLEDs because of the ability of thin monitors and flexible shape with low power intake[13-15]. In this text, for the primary time, the OLED source has been installed with a transparent optical antenna by the author. This antenna is integrated into OLED sources. OLEDs will operate as data wireless and a light source for the proposed combination of 5G [12].

D. Optical transparency:

The invisibility of the antenna is calculated by the percentage of the patch region radiating. Using the following equation, we calculate the optical transparency of the proposed antenna [16].

$$OT = \left[\frac{L_{ptch}W_{ptch} - e(XL_{ptch} + YW_{ptch}) + e^2XY}{L_{ptch}W_{ptch}} \right] \times 100 \quad (1)$$

Here,

X = Number of lines parallel to the length of the patch

Y = Number of lines orthogonal to the length of the patch

e = Thickness between two consecutive cells

TABLE-1: PARAMETERS FOR OPTICAL TRANSPARENCY

| Parameters | Values (mm) |
|------------|-------------|
| L_{ptch} | 1.39 |
| W_{ptch} | 3.21 |
| e | 0.014 |
| X | 12 |
| Y | 0 |

By inserting the values given in the table and calculating the optical transparency through the given equation, we get the antenna's conceptual optical transparency of 95%.

E. Antenna integration in OLED structure:

The proposed antenna is integrated into the OLED structure, a sandwiched structure containing four layers, each of different materials. Fig. 7 shows the antenna that is integrated into the OLED light source. The dimensions of the OLED structure are $130.2 \times 47.8 \text{ mm}^2$. It is made up of 4 layers. Layer 1 is made of glass whose thickness is 215 nm . The thickness is 150 nm for Indium Tin Oxide (ITO) at Layer 2. Layer 3 is of polymer whose thickness is 270 nm . Layer 4 is an OLED cathode that is of aluminum, having a thickness of 120 nm . The proposed antenna is placed at the corner when the four layers are piled up on the front face of OLED.

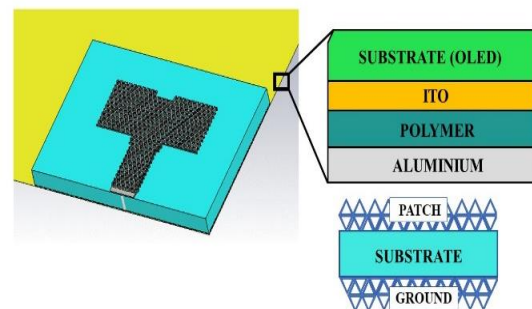


Fig. 7. The structure of OLED source with proposed antenna

IV. RESULTS AND DISCUSSION

F. Reflection coefficient (S_{11}) of a single element

This paper used Computer Simulation technology CST Microwave Studio for 5G optically transparent antenna. S_{11} defines the bandwidth and impedance matching characteristics is a notable parameter in antenna.

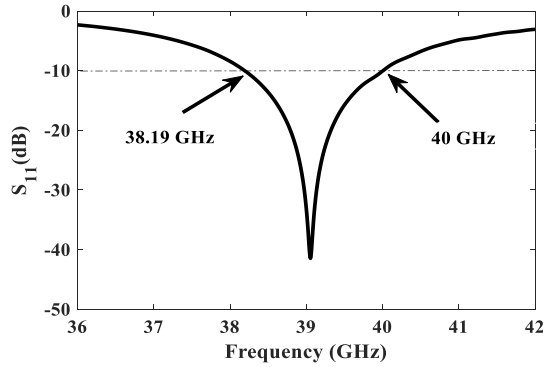


Fig. 8. S-parameter (S_{11}) of the transparent antenna proposed.

The simulated result of the reflection coefficient S_{11} is depicted in Fig. 8. The simulated results show that this antenna has a reflection coefficient S_{11} of -45dB, below -10 dB, with frequency ranging from 36GHz to 45GHz. It has a bandwidth of 1.81GHz from 38.19 GHz to 40 GHz ($S_{11} \leq -10$ dB). Considering the parametric analysis made in previous sections, we can adjust the frequency band accordingly.

G. Radiation pattern:

The antenna's radiation pattern in 3D is illustrated in Fig. 9 using CST microwave studio. After simulation, radiation with front-facing is obtained having 4.263 dB gain and 4.65 dBi directivity at 39 GHz. This obtained gain is admissible for a single antenna element. The array antenna technique will be used to make an improvement in the gain of the antenna.

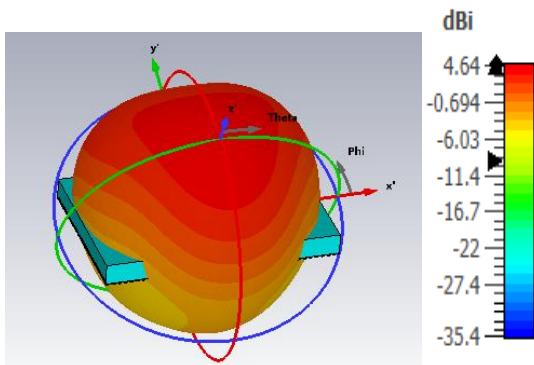


Fig. 9. Optical transparent antenna 3D radiation pattern at 39 GHz.

H. Reflection Coefficient Comparison

The reflection coefficient (S_{11}) with or without OLED of the transparent antenna is displayed in Fig. 10. Through this, we see the effect of the OLED structure on the S_{11} antenna. Therefore, the bandwidth is broadened, resonant frequency shifted to higher frequencies, and the input impedance is less suitable at 50Ω . The new frequency bandwidth is shifted away from 39GHz. For 5G communication networks, the proposed antenna has enveloped the 39 GHz band.

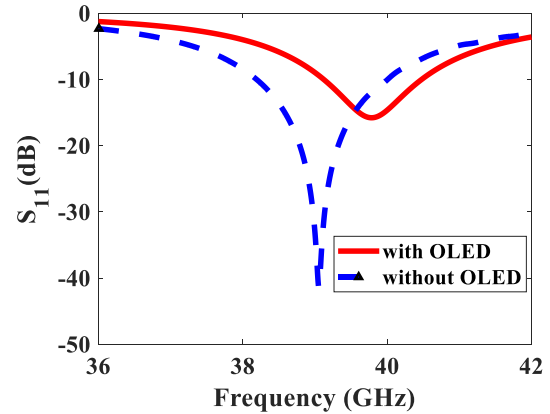


Fig. 10. The S_{11} parameter of an antenna with and without a source of OLED.

I. MIMO Parameters

1). Envelope Correlation Coordination:

The MIMO technology in 4G and 5G networks has become a compulsory means through which the data throughput of the system can be increased. The system envelope correlation coefficient was first introduced to assess the wireless diversity of the system envelope [17]. This can help the designer check the impact of the 2-element array on the system. ECC will be held out with an antenna element of more than two to have the basic concept of channel capacity.

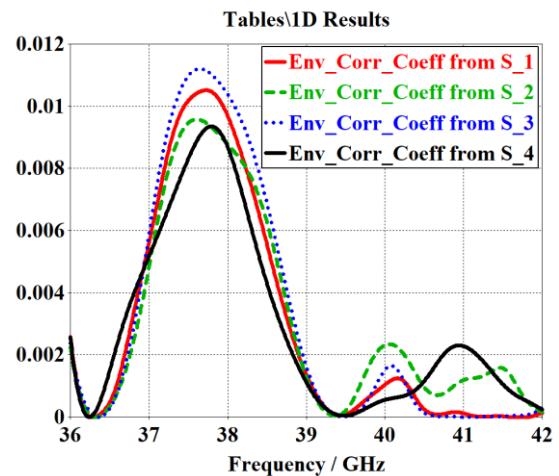


Fig.11. Envelop Correlation Coefficient of 11-element array

2). Mean effective Gain:

Due to reflection, scattering, and diffraction, some random multipath exists so sufficient accuracy cannot be evaluated for effective gain. The mobile antenna's actual performance was evaluated through experimental methods proposed by Anderson and Hansen [18]. The reference antenna and the unknown antenna's mean power can be obtained by averaging the signal levels. The effect between propagation characteristics and the power gain pattern can be measured by MEG having a mutual effect. MEG of the mobile antenna can analyze the contribution of horizontally and vertically polarized radio waves through this paper.

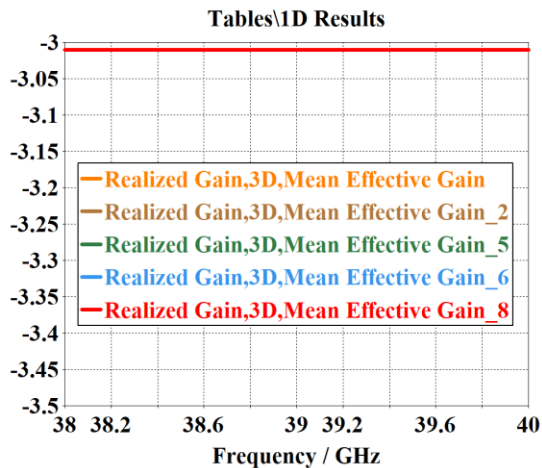


Fig. 12. Mean Effective Gain of the 11-element array.

V. CONCLUSION

A new antenna optically transparent for the fifth-generation network is demonstrated in this paper. The optical transparent antenna's patch and ground are made up of micrometric copper isosceles triangle cells. The operating frequency of our antenna is 39 GHz, from 38.19 GHz to 40 GHz, with a bandwidth of 1.81 GHz. By adjusting the micrometric triangle cells, this band is obtained. The transparency of the element radiating is calculated at approximately 95%. This transparent antenna is installed on an OLED source. After integrating the antenna into OLED, the radiation and electrical characteristics are less affected.

REFERENCES

- [1] Lucky, R.W., J. Eisenberg, and N.R. Council, *Renewing US telecommunications research*. 2006: National Academies Press.
- [2] Green, R.B., et al., *Optically transparent antennas and filters: A smart city concept to alleviate infrastructure and network capacity challenges*. IEEE Antennas and propagation magazine, 2019. 61(3): p. 37-47.
- [3] Nations, U., *Revision of world urbanization prospects*. United Nations: New York, NY, USA, 2018. 799.
- [4] Joss, S., et al., *The smart city as global discourse: Storylines and critical junctures across 27 cities*. Journal of urban technology, 2019. 26(1): p. 3-34.
- [5] Monserrat, J.F., et al., *METIS research advances towards the 5G mobile and wireless system definition*. EURASIP Journal on Wireless Communications and Networking, 2015. 2015(1): p. 1-16.
- [6] Al-Falahy, N. and O.Y. Alani, *Technologies for 5G networks: Challenges and opportunities*. IT Professional, 2017. 19(1): p. 12-20.
- [7] Klaine, P.V., et al., *A survey of machine learning techniques applied to self-organizing cellular networks*. IEEE Communications Surveys & Tutorials, 2017. 19(4): p. 2392-2431.
- [8] El Halaoui, M., et al., *Multiband planar inverted-F antenna with independent operating bands control for mobile handset applications*. International Journal of Antennas and Propagation, 2017. 2017.
- [9] Park, J., et al., *An optically invisible antenna-on-display concept for millimeter-wave 5G cellular devices*. IEEE Transactions on Antennas and Propagation, 2019. 67(5): p. 2942-2952.
- [10] Lee, S.Y., et al. *Electrical characterization of highly efficient, optically transparent nanometers-thick unit cells for antenna-on-display applications*. in *2018 IEEE/MTT-S International Microwave Symposium-IMS*. 2018. IEEE.
- [11] Hong, W., et al., *Optically invisible antenna integrated within an OLED touch display panel for IoT applications*. IEEE Transactions on Antennas and Propagation, 2017. 65(7): p. 3750-3755.
- [12] El Halaoui, M., et al. *An optically transparent antenna integrated in OLED light source for 5G applications*. in *2020 IEEE International Conference on Environment and Electrical Engineering and 2020 IEEE Industrial and Commercial Power Systems Europe (EEEIC/I&CPS Europe)*. 2020. IEEE.
- [13] Salameh, F., et al., *Modeling the luminance degradation of OLEDs using design of experiments*. IEEE Transactions on Industry Applications, 2019. 55(6): p. 6548-6558.
- [14] Azrain, M., et al., *Failure mechanism of organic light emitting diodes (OLEDs) induced by hygrothermal effect*. Optical Materials, 2019. 91: p. 85-92.
- [15] Al Haddad, A., et al. *Parametric degradation model of OLED using Design of Experiments (DoE)*. in *2019 IEEE 12th International*

- Symposium on Diagnostics for Electrical Machines, Power Electronics and Drives (SDEMPED)*. 2019. IEEE.
- [16] Yasin, T., *Analysis and design of highly transparent meshed patch antenna backed by a solid ground plane*. Progress In Electromagnetics Research M, 2017. 56: p. 133-144.
- [17] R. G. Vaughan, J. B. Andersen, "Antenna diversity in mobile communications", IEEE Trans. Veh. Technol., vol. VT-36, pp. 147-172, Nov. 1987.
- [18] J. Bach Andersen and F. Hansen, "Antennas for VHF/UHF personal radio: A theoretical and experimental study of characteristics and performance," IEEE Trans. Veh. Technol., vol. VT-26, no. 4, pp. 349-357, 1977.
- [19] A GSA Executive Report from Ericsson, Huawei and Qualcomm, "The road to 5G: Drivers, applications, requirements and technical development," Global Mobile Suppliers Assoc., Ericsson, Stockholm, Sweden, GSA Executive Rep., Nov. 2015.